# Thermal decomposition synthesis and magnetic properties of crystalline zinc oxide powders

**C Wisetrinthong [1], S Pinitsoontorn[2] P Kidkhunthod[3] and K Wongsaprom[1,*]**
[1]Department of Physics, Faculty of Science, Mahasarakham University, 44150, Mahasarakham
[2]Department of Physics, Faculty of Science, KhonKaen University, 40002, Khon Kaen
[3]Synchrotron Light Research Institute (Public Organization), 111 University Avenue, Muang District, 30000, Nakhon Ratchasima

*E-mail: wkwanruthai@gmail.com

**Abstract**. Crystalline zinc oxide powders are prepared by a direct thermal decomposition of zinc nitrate hexahydrate in air at 500 ºC for 2 h. The thermal behavior of zinc precursor compound was studied using TG-DTA analysis in order to define the ZnO formation temperature. The structure of the calcined sample was characterized by X-ray diffraction (XRD). The XRD result indicates that the sample has a pure phase with ZnO wurzite structure. The morphology and elemental composition have been identified through SEM and EDX analyses. The oxidation state of ZnO sample was investigated using X-ray absorption near-edge spectroscopy (XANES). The ZnO sample reveals ferromagnetic behavior with the magnetization of ~0.50 emu/g at 15 kOe. Our results indicate that room-temperature ferromagnetism of ZnO is intrinsic.

## 1. Introduction

Oxide-based diluted magnetic semiconductors (O-DMSs) such as $SnO_2$, $In_2O_3$, $CeO_2$ and $TiO_2$ doped with magnetic transition metal elements have recently attracted much attention due to their potential use in spintronic devices and other applications [1-4]. These O-DMSs are optically transparent and exhibit room and above room temperature ferromagnetism. Among these metal oxides, zinc oxide (ZnO) is n-type wide band gap semiconductor ($E_g$ = 3.37 eV) and large exciton binding energy (60 meV) [5]. Thus, these unique properties make ZnO a promising candidate for important applications, especially in optics and optoelectronics [6]. Recently, ZnO doping by 3*d* transition metal has been reported to reveal room and above room temperature ferromagnetism [7-8]. In addition, undoped ZnO with various morphologies are also exhibited room temperature ferromagnetism [9-10]. Chen et al. [9] reported room temperature in ZnO pellets. The author suggested that the ferromagnetism is originated mainly by surface oxygen vacancies and hydrogenation. Sun et al. [10] fund that room temperature ferromagnetism existed in porous ZnO prepared by thermal decomposition method with the largest saturation magnetization of about 0.026 emu/g. They suggested that the correlation between magnetism and point defect demonstrate that the concentration of oxygen vacancies. At present, only few studies have been reported on the magnetic properties of crystalline ZnO powders. However, the origin of ferromagnetism in ZnO is not clear at the moment. Therefore, it is of great interest to study the ferromagnetic properties in pure ZnO as it can be further studied for basic science and the understanding of future spintronic devices.

In this paper, we report a successful synthesis and magnetic properties of crystalline ZnO powder through thermal decomposition. This method compared with other techniques reveals advantages such

as the lack of high pressure conditions, multiple reaction steps, specific instrumentation or toxic byproducts. The crystalline ZnO powders were characterized by XRD, SEM and EDX. The magnetic properties were investigated using VSM at below and room temperature. Furthermore, importantly, an X-ray Absorption Spectroscopy (XAS) including X-ray Absorption Near Edge Structure (XANES) is performed and played an important role to confirm and understand in term of qualitative Zn oxidation states causing a magnetic property in these such samples.

## 2. Experimental procedure

In this study, zinc nitrate hexahydrate (99.8%, Sigma-Aldrich) was used as starting material. In a typical procedure, 1g of $Zn(NO_3)_2.6H_2O$ was dissolved in deionized water (DI water) at a ratio of 5:1 (volume (ml)/weight (g)) of DI water to total nitrate salts. The mixed solution was stirred with a magnetic stirrer at room temperature for 60 min, and was thermally decomposition in a box-furnace at 500 $^oC$ in air for 2 h obtain ZnO powders. To understand thermal stability, decomposition temperature and mechanism of thermal decomposition, precursors of the mixed nitrate in DI water was characterized by TG-DTA (TA Inc., SDT 2960) at 10 $^oC\ min^{-1}$ from 30 to 500 $^oC$. The calcined samples were characterized for crystal phase indentification by powder X-ray diffraction (XRD) using a Philips X-ray diffractometer (XRD, Bruker-D8 advanced X-ray diffractometer) with CuKα radiation ($\lambda = 0.15418$ nm). Scanning electron microscopy (SEM, LEO-1450VP) was used to observe the surface morphology of sample. Elemental analysis of sample was determined by Desktop Scanning Electron Microscopes (MiniSEM, SEC-SNE-4500M). X-ray absorption Near Edge Structure (XANES) spectra of Fe *K*-edge were measured at room temperature in transmission mode using a Ge(220) double-crystal monochromator with an energy resolution ($\Delta E/E$) of $2 \times 10^{-4}$ at the SUT-NANOTEC-SLRI XAS Beamline (BL 5.2) (electron energy of 1.2 GeV; bending magnet; beam current 80 – 150 mA; 1.1 to $1.7 \times 10^{11}$ photon $s^{-1}$) at the Synchrotron Research Institute in Nakhon Ratchasima, Thailand [11]. The magnetic measurements were performed at below and room temperature using a vibrating sample magnetometer (Versa Lab VSM, Quantum Design).

## 3. Results and discussion

The TG-DTA result of the $Zn(NO_3)_2.6H_2O$ precursor in Figure 1 shows that precursor lost its weight in two different steps. The first weight loss step (~40.5%) is between ~30 to 215 $^oC$ with an endothermic peak at 94 $^oC$ can be attributed to the thermal dehydration of water in the precursor. The second step of weight loss (~34%) is between 215-355 $^oC$ with small endothermic centered at 225 and 344 $^oC$ and an exothermic peaks at 281 $^oC$, which is associated probably with the starting of nitrate decomposition of oxygen atoms from $(NO_3)_2$ to the ZnO network. The main exothermic effect between 355 and 500 $^oC$ with maximum at 363 $^oC$ attributed to the final transformation of the precursor into ZnO product [6].

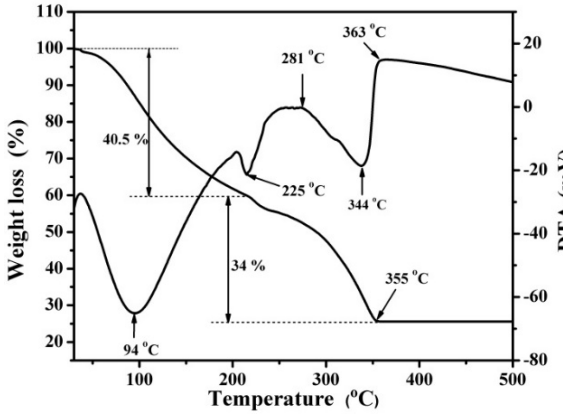


**Figure 1.** TG-DTA curves of the thermal decomposition of the $Zn(NO_3)_2 \cdot 6H_2O$ at a heating rate of 10 $^oC$/min

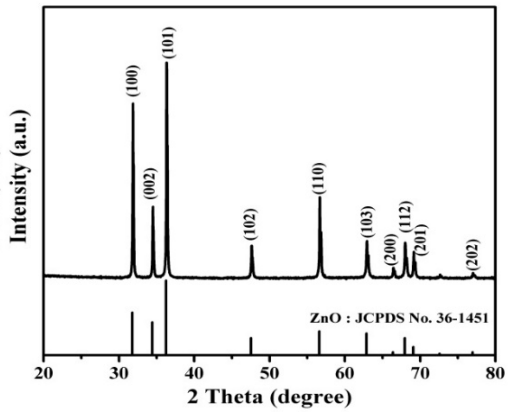


**Figure 2**. XRD pattern of ZnO powders calcined at 500 $^oC$

The structure of the nanocrystalline ZnO sample were primary examined by XRD. XRD patterns of the sample in Figure 2 show the single phase of ZnO hexagonal wurtzite structure as compared to the standard data (JCPDS 36-1451). There is no diffraction peak originating from impurity phase in the

XRD pattern. The crystallite size of the sample was calculated from X-ray line broadening of the peak at (100), (002) and (101) planes using Scherrer's equation. The crystallite size of the ZnO sample was obtained to be 71.7±3.9 nm. The elemental composition and morphology of ZnO were investigated by EDX and SEM in Figure 3. The sample reveals peaks of Zn and O. No evidence of impurity phases was identified by XRD and EDX. Moreover, the presence of C, Cu and Au came from carbon tap, copper in the coin and coated Au over the sample, respectively. These results indicate that the room temperature ferromagnetism of the sample should not come from the secondary phase. The morphology of the ZnO sample was studied by FESEM as shown in an inset of Figure 3. The SEM micrograph shows agglomerated particles. The particles tend to agglomerate during synthesis or delivery process due to their high surface area and surface energy [12].

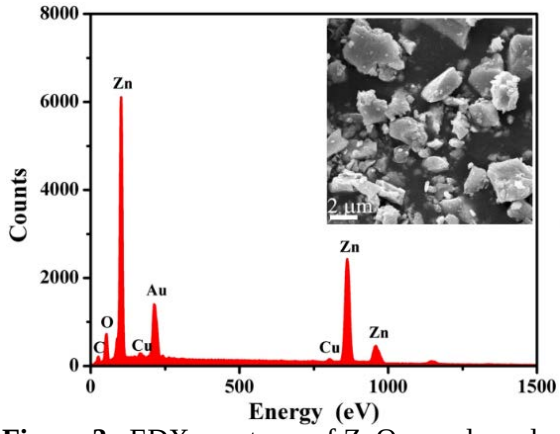


**Figure 3.** EDX spectrum of ZnO sample and the inset show the SEM image of ZnO sample

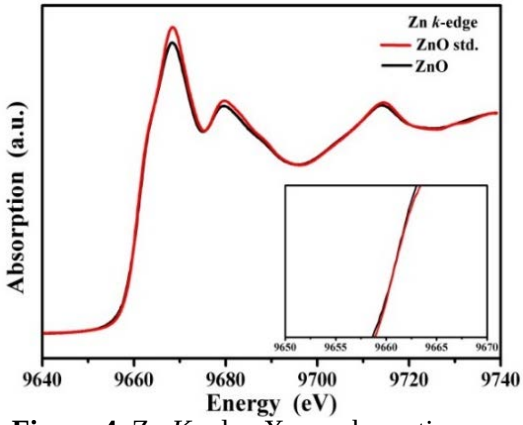


**Figure 4.** Zn *K*-edge X-ray absorption near-edge structure for ZnO standard and XANES spectra of ZnO sample

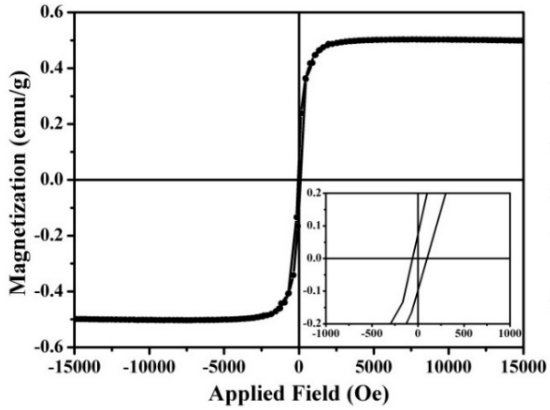


**Figure 5.** Magnetization of ZnO sample as a function of field at 300 K

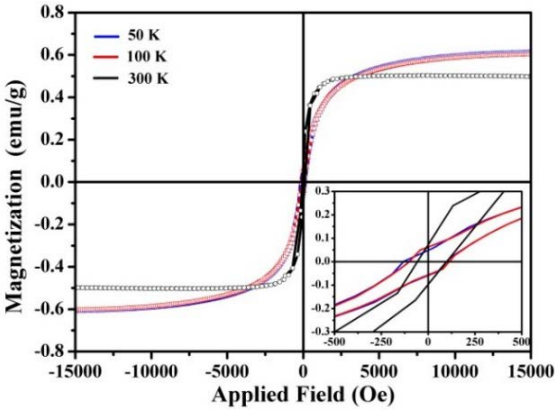


**Figure 6.** Magnetization of ZnO sample as a function of field at 50 K, 100 K and 300 K

In order to further determine the origin of room temperature ferromagnetism, the series of Zn K-edge of XANES were further measured to examine the electronic structure and various chemical states of Zn element in the sample. The background correction and normalization also the absorption edge energy was evaluated using Athena software in the IFEFFIT package [13, 14]. Figure 4 shows the Zn K spectra of ZnO sample comparing with the known $Zn^{2+}$ standards (commercial ZnO). The spectrum of ZnO sample exhibits the features and energy edges at 9660.78 eV which is similar to the standard ZnO. This result is consistent with the preceding XRD analysis. In more detail, the white-line peak position occured around 9665 eV reflects the summed intensities of electron transitions from Zn-1s to Zn-4p orbital. The

decrease of peak's intensity of ZnO sample compared with the ZnO standard implies an oxygen defect or vancancy occurring in the prepared ZnO sample [15]. Figure 5 and Figure 6 show the field dependence of magnetization (M-H curve) of ZnO sample obtained from VSM measurement (with the removal of any diamagnetic contribution) at 50, 100 and 300 K. The saturation magnetization ($M_s$) of the sample at 300, 100 and 50 K are ~0.499, 0.602 and 0.603 emu/g, respectively. The values of coercivity ($H_c$) of the sample measured at 300, 100 and 50 K are ~77.9, 106.8 and 114.2 Oe, respectively. The origin of room temperature ferromagnetism in ZnO system possibly results from defects created by doping, implantation or annealing. In addition, low crystalline quality, i.e., strain and grain boundaries as well as excess of Zn due to oxygen vacancies or Zn interstitials appear to play a key role in development of ferromagnetism [16]. The XRD and XANES results imply that the ZnO sample has a single wurtzite phase without any secondary phases. Therefore, the intrinsic ferromagnetism in ZnO system can be explained by the presence of oxygen vacancies on the surface. It is possible that oxygen vacancies can create magnetic moments on neighboring Zn ions [9].

## 4. Conclusion

The synthesis of ZnO nanocrystalline powders with crystallite size of ~ 71.7±3.9 nm by a simple thermal decomposition method were studied in this paper. The sample reveals single phase wurtzite structure of ZnO. XANES spectra showed that Zn atom in the sample have oxidation states of 2+ in the structure. A ferromagnetic exchange mechanism in ZnO sample was thought to be induce by oxygen vacancies. These results may be useful for producing magnetic memory devices.


## Acknowledgments

The authors would like to thank the Synchrotron Light Research Institute (BL5.2) (Public Organization), Nakhon Ratchasima, Thailand for XAS facilities. This Research was financially supported by Mahasarakham University, Thailand.


## References


[1] Fitzgerald C B, Venkatesan M, Douvalis A P., Huber S, Coey J M D and Bakas T 2004 *J. Appl. Phys.* **95** 7390
[2] Yan S, Ge S, Zuo Y, Qiao W and Zhang L 2009 *Scripta Meter.* **61** 387
[3] Phokha S, Pinitsoontorn S and Maensiri S 2012 *J. Appl. Phys.* **112** 113904
[4] Martinez B, Sandiumenge F, Balcells Ll, Arbiol J, Sibieude F and Monty C 2005 *Appl. Phys. Lett.* **86** 103113
[5] Flores-Carrasco G, Carrillo-Lopez J, Martinez-Martinez R, Espinosa-Torres N D, Munoz L, Milosevic O and Rabanal M E 2016 *Appl. Phys. A* **122** 173
[6] Fu H K, Cheng C L, Wang C H, Lin T Y and Chen Y F 2009 *Adv. Funct. Mater.* **19** 3471.
[7] Venkatesan M, Stamenov P, Dorneles L S, Gunning R D, Bernoux B and Coey J M D 2007 *Appl. Phys. Lett.* **90** 242508
[8] Fukumura T, Jin Z and Kawasaki M 2001 *Appl. Phys. Lett.* **78** 958
[9] Xing et al. 2010 *Appl. Phys. Lett.* **96** 112511
[10] Ghose S, Sarkar A, Chattopadhyay S, Chakrabarti M, Das D, Rakshit T, Ray S. K. and Jana D. 2013 *J. Appl. Phys.* **114** 073516
[11] Kidkhunthod P 2017 *Adv. Nat. Sci: Nanosci. Nanotechnol.* **8** 035007
[12] Raichman Y, Kazakevich M, Rabkin E and Tsur Y 2006 *Adv. Mater.* **18** 2028
[13] Newville M 2001 *J. Synchrotron Radiat.* **8** 96
[14] Ravel B and Newville M 2005 *J. Synchrotron Rad.* **12** 537
[15] Haug J, Chasse A, Dubiel M, Eisenschmidt C, Khalid M and Esquinazi P 2011 *J. Appl. Phys.***110** 063507
[16] Potzger K, Zhou S, Grenzer J, Helm M and Fassbender J 2008 *Appl. Phys. Lett.* **92** 182504